PHYSICAL REVIEW B VOLUME 46, NUMBER 4 15 JULY 1992-II

Hyperspherical formulation of impurity-bound excitons in semiconductors

J. J. De Groote and J. E. Hornos
Instituto de Física e Química de São Carlos, Universidade de São Paulo,
13560 São Carlos, São Paulo, Brazil

H. T. Coelho
Departamento de Física, Universidade Federal de Pernambuco, 50739 Recife, Pernambuco, Brazil

C. D. Caldwell
Department of Physics, University of Central Florida, Orlando, Florida 32816

(Received 24 February 1992)

A hyperspherical formalism is shown to be an appropriate approach for the investigation of the three-particle complex corresponding to an exciton bound to a Coulomb center in a semiconductor. The ground- and excited-state potential curves and binding energies are calculated as a function of the mass ratio of the hole and electron, and the concept of a critical mass is discussed. The results that we have obtained are in very good agreement with variational calculations for several semiconductor materials.

I. INTRODUCTION

The properties of excitons bound to imperfections in semiconductors have been the subject of numerous theoretical[1–5] and experimental[1,6–8] investigations. Bonding can occur to both neutral and ionized impurities. The simplest form of the complex has a molecular-like structure, which gives rise to several lines in the spectra in addition to those originating from the free exciton. More complicated behavior can arise from clustering[9] of excitons into biexcitons or when the particles are subjected to axial external fields (quantum wells)[10] or confinement fields (quantum dots).[11] While a simple hydrogenic approach is adequate for the description of the properties of the free exciton, bond formation, clustering, and the presence of external fields requires a more sophisticated mathematical approach to treat the many-body effects.

Spherical coordinates in higher dimensions, normally called hyperspherical coordinates (HC), have been used frequently to solve few-body quantum problems in strong-interaction physics.[12] The same approach has also been used in some instances in atomic and molecular physics[13–18] to obtain wave functions for the three-body problem. Normally the use of HC leads to a difficult problem of a coupled system of differential equations of infinite dimension. This difficulty becomes even more severe if Coulomb forces are present.

A well-established and, in essence, exact procedure for handling physical systems within the HC scheme is the hyperspherical adiabatic approach (HAA). The literature[12–18] is full of examples illustrating the use of the HAA from the atomic to the nuclear scale. This approach is similar to the Born-Oppenheimer approximation used to calculate vibrational potential curves for diatomic molecules. In the application of this technique, the Schrödinger equation in HC is solved at each fixed hyperradius R, the coordinate that describes the overall size of the system, to generate a family of effective-potential curves $U_\lambda(R)$: The integer λ characterizes the set of orbital angular momenta of the various particles in the system. For short-range forces, $U_\lambda(R)$ is successfully obtained by diagonalization procedures.[12] However, for long-range forces this procedure does not prove to be practical. The rapidly oscillating Jacobi polynomials, the hyperspherical harmonic functions that are the analytic solutions to the radial equation at small R, give rise to instabilities with slow convergence. Slow convergence also results from the fact that the asymptotic solutions are not easily expanded in terms of hyperspherical harmonics.

One approach to removing this difficulty is through the introduction of another variable, $z=\tan(\alpha/2)$, where α is one of the hyperspherical angles in the three-body problem. The resulting differential equation in terms of z can then be written in canonical form and does not require an expansion in oscillating harmonic functions. Further improvement of the convergence can be obtained by incorporating the properties of the differential equations in the small and large R limits in the initial ansatz, thereby further simplifying the form of the canonical equation. Once $U_\lambda(R)$ is known, the radial equation for R can be solved to obtain the eigenenergies of the system.

The aim of this paper is to introduce the HAA to the realm of problems in exciton physics and to show that it forms an appropriate framework for the understanding of the difficulties outlined above. The specific system that will be addressed is the bonding of the exciton to an ionized donor. In the course of the calculation we will make use of a recently proven set of basic inequalities[19] that provide a lower bound–upper bound relation for the ground-state energies of this system. The concept of a critical mass is also discussed in light of the exact method presented in this work. It seems that its existence is linked to the accuracy of the theoretical calculation.

This paper is organized in the following manner. In Sec. II we present the general formalism as it exists in the literature. A method for obtaining potential curves similar to the Born-Oppenheimer approximation is given in Sec. III. The calculation of the binding energies and wave functions will be the subject of Sec. IV. Finally, in Sec. V we will give the conclusions. Two appendixes are also included.

II. THE EFFECTIVE-MASS MODEL IN THE HYPERSPHERICAL APPROACH

The binding of an exciton to an ionized impurity can be properly described in the effective-mass model by the Schrödinger equation for the motion of the electron-hole pair in the field of a fixed-impurity center of change Ze, as

$$\left[-\frac{\hbar^2}{2m_e^*}\nabla_e^2-\frac{\hbar^2}{2m_h^*}\nabla_h^2-\frac{Ze^2}{\epsilon|\mathbf{r}_e|}+\frac{Ze^2}{\epsilon|\mathbf{r}_h|}-\frac{e^2}{\epsilon|\mathbf{r}_e-\mathbf{r}_h|}-E\right]\psi(\mathbf{r}_e,\mathbf{r}_h)=0\ . \qquad (1)$$

The effects of the many-body interactions are represented in the effective masses of the electron m_e^* and the hole m_h^* and in the static dielectric constant ϵ of the material. Here $\mathbf{r}_e$ and $\mathbf{r}_h$ are the electron and hole distances from the ionized donor impurity, respectively. Instead of using the independent particle coordinates (r_e,θ_e,φ_e) and (r_h,θ_h,φ_h), we solve Eq. (1) by making a transformation to hyperspherical coordinates, as shown in a general procedure given in Appendix A. In Appendix A, if we set $m_1\rightarrow\infty$, $m_2=m_e^*$, $m_3=m_h^*$, $q_1=Ze$, $q_2=-e$, and $q_3=e$, and define $m=m_h^*/m_e^*$, we obtain

$$\left[\frac{\partial^2}{\partial R^2}+\frac{\frac{1}{4}-U(R,\Omega)}{R^2}+\varepsilon\right]\Psi(R,\Omega)=0\ , \qquad (2)$$

where Ψ, the renormalized wave function, and $U(R,\Omega)$ are defined in Appendix A.

The three-body Coulombic interaction $\hat{V}(\alpha,\theta)$ is given by

$$\hat{V}(\alpha,\theta)=-\left[\frac{m_e^*}{\mu}\right]^{1/2}\frac{Ze^2}{\epsilon\sin\alpha}+\left[\frac{m_h^*}{\mu}\right]^{1/2}\frac{Ze^2}{\epsilon\cos\alpha}-\left[\frac{m_e^*}{\mu}\right]^{1/2}\frac{e^2}{\epsilon}\left[\sin^2\alpha+\frac{\cos^2\alpha}{m}-\frac{\sin(2\alpha)\cos\theta}{\sqrt{m}}\right]^{-1/2}, \qquad (3)$$

where

$$\hat{v}(\alpha,\theta)=(2\mu/\hbar^2)\hat{V}(\alpha,\theta)\ . \qquad (4)$$

We will seek solutions to Eq. (2) that are characterized by a constant-total angular momentum L and projection M. Then, the solution to the hyperspherical equations proceeds in the following way. First, a set of eigenvalues for the operator U is determined as a function of the radial coordinate R according to

$$U(R,\Omega)\Phi_\lambda(R,\Omega)=U_\lambda(R)\Phi_\lambda(R,\Omega)\ , \qquad (5)$$

where the index λ denotes the set of integer labels (L,M,l,l_e,l_h). The integers l, l_e, and l_h derive from the characterization of the angular solution of Eq. (5) in the case of $R=0$. In this limit the equation can be solved exactly,[13] yielding eigenvalues

$$U_\lambda(0)=(2l+l_e+l_h+2)^2\ , \qquad (6)$$

and eigenfunctions

$$\Phi_\lambda(0,\Omega)=\sum_{l_e',l_h'}(\sin\alpha)^{l_e'+1}(\cos\alpha)^{l_h'+1}\times P_l^{l_e'+1/2,\,l_h'+1/2}(\cos(2\alpha))\mathcal{Y}_{l_e'l_h'}^{LM}(\hat{\xi}_e,\hat{\xi}_h)\ , \qquad (7)$$

where P and $\mathcal{Y}$ are the Jacobi polynomials and the generalized spherical harmonics, respectively. Once the eigensolutions of Eq. (5) have been obtained, they can then be used as a basis for the expansion of the wave function Ψ as

$$\Psi(R,\Omega)=\sum_\lambda F_\lambda(R)\Phi_\lambda(R,\Omega)\ . \qquad (8)$$

In the second step we return to the Schrödinger equation in order to obtain a set of radial equations

$$\left[\frac{d^2}{dR^2}+\frac{\frac{1}{4}-U_\lambda(R)}{R^2}+\varepsilon\right]F_\lambda(R)+\sum_{\lambda'}W_{\lambda\lambda'}(R)F_{\lambda'}(R)=0\ , \qquad (9)$$

where

$$W_{\lambda\lambda'}(R)=2P_{\lambda\lambda'}(R)\frac{d}{dR}+Q_{\lambda\lambda'}(R)\ , \qquad (10)$$

and

$$P_{\lambda\lambda'}(R)=\left\langle\Phi_\lambda\left|\frac{d\Phi_{\lambda'}}{dR}\right.\right\rangle=\int_\Omega\Phi_\lambda^*\frac{d\Phi_{\lambda'}}{dR}d\Omega\ , \qquad (11)$$

$$Q_{\lambda\lambda'}(R)=\left\langle\Phi_\lambda\left|\frac{d^2\Phi_{\lambda'}}{dR^2}\right.\right\rangle=\int_\Omega\Phi_\lambda^*\frac{d^2\Phi_{\lambda'}}{dR^2}d\Omega\ . \qquad (12)$$

Solutions to the set of Eq. (9) can be obtained within various approximations. The simplest of these, the extreme adiabatic approximation (EAA), neglects all coupling terms given by Eqs. (10)–(12). The energies calculated in this approximation form a lower bound to the exact value.[19] Inclusion of the diagonal term $W_{\lambda\lambda}(R)$ gives the so-called uncoupled adiabatic approximation (UAA). While satisfactory results can be obtained in either of these limits, a systematic improvement can be achieved by the successive inclusion of additional off-diagonal coupling terms, giving rise to the coupled adiabatic approximation (CAA). The ground-state binding energies obtained in these adiabatic approximations satisfy the basic inequalities[19]

$$\varepsilon_{\mathrm{EAA}}\leq\varepsilon\leq\varepsilon_{\mathrm{CAA}}\leq\varepsilon_{\mathrm{UAA}}\ . \qquad (13)$$

III. POTENTIAL CURVES AND CHANNEL FUNCTIONS

In the solution of Eq. (5) to obtain the eigenpotentials $U_\lambda(R)$, it is necessary to develop an efficient procedure for handling the numerical calculations such that the $U_\lambda(R)$'s are precisely obtained for the entire range of R. In order to achieve this in an efficient way, we begin by examining the kinetic term of Eq. (A7). That term has poles at $\alpha=0$, $\pi/2$ that are independent of the masses of the system. On the other hand, the Coulomb interaction term, given by Eq. (3), has poles at $\alpha=0$ and at $(\theta,\alpha)=(\pi,\alpha_+)$ and $(0,\alpha_-)$, where $\tan\alpha_\pm=\eta_\pm$. In Appendix A, if we set $m_1=\infty$, we obtain $\alpha_+=\pi/2$ and $\tan\alpha_{-1}=1/\sqrt{m}$. Let us define $\alpha_-=\alpha_c$. Then, the potential curves are obtained by considering regular solutions in the two regions $0\le\alpha\le\alpha_c$ and $\alpha_c\le\alpha\le\pi/2$ and imposing continuity conditions at those boundary points. Notice that the presence of the poles at $\alpha=0$ and $\alpha=\pi/2$ corresponds to the ionization limits, either the electron is at infinity or the hole is at infinity.

In this kind of investigation it is important to select the appropriate angles and the corresponding harmonic for use as a basis for the problem. There exist different ways to select those angles: these have been well studied by Smirnov and Shitikova.[20] Each possibility is identified with a possible chain in which the group O(6) can have its representation decomposed. As we seek solutions that are characterized by the total value of the angular momentum L, the most appropriate basis for the expression of the angular dependence is given by the two-particle spherical harmonics. Thus, we have chosen the chain

$$\begin{array}{ccccc} O(6) & \supset O(3)\times & O(3)\supset & O(3)\supset & O(2) \\ \downarrow & \downarrow & \downarrow & \downarrow & \downarrow \\ \{n\ell_e\ell_h\} & \{\ell_e\} & \{\ell_h\} & \{L\} & \{M\}, \end{array} \qquad (14)$$

which corresponds to the use of the three-dimensional two-particle spherical harmonics. The channel functions, i.e., the solutions to the eigenvalue equation (5) for each value of R, are then written as

$$\Phi_\lambda(R,\Omega)=\sum_{l_e,l_h}(\sin\alpha)^{l_e+1}(\cos\alpha)^{l_h+1} \times\mathcal{Y}^{LM}_{l_el_h}(\hat{\xi}_e,\hat{\xi}_h)\mathcal{G}^\lambda_{l_el_h}(R,\alpha)\ , \qquad (15)$$

where $\mathcal{Y}^{LM}_{l_el_h}$ is the usual two-particle coupled-orbital angular-momentum function ($|l_e-l_h|\le L\le l_e+l_h$, and $M=m_e+m_h$). The basis functions $\mathcal{G}^\lambda_{l_el_h}(R,\alpha)$ at each R are obtained from the solution of Eq. (5). The strong singularities at $\alpha=0,\pi/2$ are smoothed by the presence of the functions $\sin\alpha$ and $\cos\alpha$ in Eq. (15).

The motivation for the choice given by Eq. (15), instead of other possibilities (such as Euler angles[14] or the canonical form used in nuclear physics[12]), is the following. The decomposition in the two O(3) groups preserves the individuality of the effective particles with respect to the angular motion in the (θ_e,φ_e), (θ_h,φ_h) manifolds. However, the introduction of the variables α and R will account for the collective effects.

We note that the function $\mathcal{G}^\lambda_{l_el_h}(R,\alpha)$ in Eq. (15) was not further expanded in any basis. In this respect our approach differs from the usual techniques which are based on an expansion using orthonormal polynomials[12,14,16,17] or another[14] set of functions with faster convergence properties. As discussed elsewhere,[13] our approach seems to be the most appropriate for long-range forces. For Coulombic systems the use of other approaches generates a number of problems, such as slow convergence, incorrect asymptotic behavior, nonorthonormal sets, etc. In order to avoid these problems we shall solve directly the infinite set of differential equations obtained by substituting Eq. (18) into Eq. (11), namely

$$\left\{\frac{d^2}{d\alpha^2}+2[(l_e+1)\cot\alpha-(l_h+1)\tan\alpha]\frac{d}{d\alpha}-U_\lambda(R)-(l_e+l_h+2)^2\right\}\mathcal{G}^\lambda_{l_el_h}(R,\alpha)-R\sum_{l'_e,l'_h}\tilde{v}^{LM}_{l_el_hl'_el'_h}(\alpha)\mathcal{G}^\lambda_{l'_el'_h}(R,\alpha)=0\ , \qquad (16)$$

where

$$\tilde{v}^{LM}_{l_el_hl'_el'_h}(\alpha)=(\sin\alpha)^{l'_e-l_e}(\cos\alpha)^{l'_h-l_h}\langle\mathcal{Y}^{LM}_{l_el_h}|\hat{v}|\mathcal{Y}^{LM}_{l'_el'_h}\rangle\ . \qquad (17)$$

The explicit expression for $\langle\hat{v}\rangle$ is given in Appendix B. In the solution of Eq. (16) it is necessary to keep in mind the symmetries imposed in the hyperspherical harmonic functions $\mathcal{G}^\lambda_{l_el_h}(R,\alpha)$. A discussion of this point is given, for example, in Refs. 12 and 13. Equation (16) is solved in the region $0\le\alpha\le\alpha_c$. A totally analogous procedure applied to the region $\alpha_c\le\alpha\le\pi/2$ leads to a similar equation.

We demonstrated earlier[13] that instabilities which hamper the successful solution of the eigenvalue equation for long-range forces can be avoided by the introduction of another variable $z=\tan(\alpha/2)$. This allowed us to rewrite the eigenvalue equation for $U_\lambda(R)$ in the "canonical" form, i.e., all coefficients are simple rational functions of the variable z. Therefore, a power series solution could be implemented via a finite recursion formula. We will exploit the same technique in the solution of the eigenvalue equation, Eq. (16). To this end we introduce the variable $z=\tan(\alpha/2)$ in the two regions. The two equations in each region are analogous and take the form

$$\left[\frac{d^2}{dz^2}+\mathcal{P}_{l_el_h}(z)\frac{d}{dz}+\mathcal{Q}_{l_el_h}\right]\mathcal{G}^\lambda_{l_el_h}(R,z) +R\sum_{l'_el'_h}\mathcal{R}_{l_el'_el_hl'_h}\mathcal{G}^\lambda_{l'_el'_h}(R,z)=0\ , \qquad (18)$$

where

$$\mathcal{P}_{l_e l_h}(z)=\frac{2}{1+z^2}\left[z+\frac{(l_e+1)(1-z^2)}{z}\right.$$
$$\left.-\frac{4(l_h+1)z}{1-z^2}\right], \tag{19}$$

$$\mathcal{Q}_{l_e l_h}(z)=-4[(l_e+l_h+2)^2+U_\lambda(R)]/(1+z^2)^2$$
$$+\left[\frac{m_e^*}{\mu}\right]^{1/2}\frac{Ze^2}{\epsilon}\frac{2R}{z(1+z^2)}$$
$$-\left[\frac{m_h^*}{\mu}\right]^{1/2}\frac{Ze^2}{\epsilon}\frac{4R}{(1+z^2)(1-z^2)}, \tag{20}$$

and

$$\mathcal{R}_{l_e l_e' l_h l_h'}(z)=\frac{4}{(1+z^2)^2}\left[\frac{2z}{1+z^2}\right]^{l_e'-l_e}$$
$$\times\left[\frac{1-z^2}{1+z^2}\right]^{l_h'-l_h}\left[\frac{m_e^*}{\mu}\right]^{1/2}\frac{e^2}{\epsilon}\Delta_{l_e l_e' l_h l_h'}. \tag{21}$$

Equation (18) can be solved in each region of space through a series expansion in the variable z. In contrast to the simpler helium system with two electrons, care must be taken in evaluating the series, as the angle α_c can become large for large values of the mass ratio. This implies that it may be necessary to use many more terms in the expansion to ensure convergence in one or the other region.

The solution of Eq. (18) involves the truncation of the expansion in the angular momenta l_e and l_h. However, in contrast to the situation obtained in atomic physics, the formation of the bound state for the system described here is critically dependent on the presence of the correlation. Thus, it is necessary to include many more terms in the angular expansion than the three or four which typically deliver good results in the more familiar system.

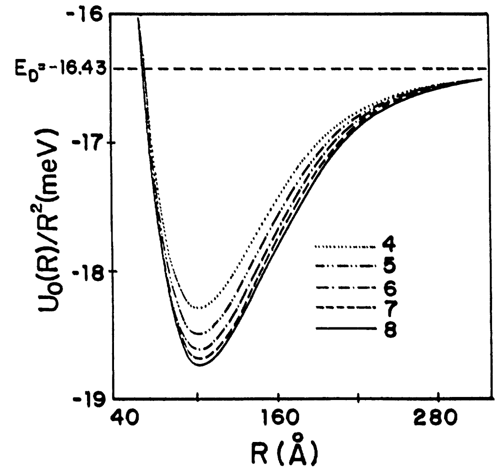

FIG. 1. Potential curves as a function of the number of angular channels for ZnSe. Graphs here are given for 4–8 channels. Note that convergence requires the use of a large number of channels in the calculation. The deeper the curve the larger the number of channels required.

In order to understand the critical role that correlation plays in the bonding of the exciton to the impurity, we compare it with the helium problem.[13] In the case of helium, a zeroth-order approximation in which the particle-particle correlation is totally neglected produces a bound state. In the case of the exciton, the neglect of the correlation (electron-hole) interaction produces a scattering system in which one particle is captured by the impurity and the other is free in the crystal. When the electron-hole interaction is turned on and a systematic inclusion of higher- and higher-angular-momentum channels is carried out, the minimum of the potential curve is uniformly lowered. As a result, the three-body system is bound together. This can be seen clearly in Fig. 1, which gives the convergence of the potential for the semiconductor ZnSe as a function of the number of angular-momentum channels used. A considerable change in the potential minimum is still taking place for the jump from four to five channels. Typically, we use eight angular-momentum channels in our calculations.

Another effect of the truncation of the number of angular-momentum channels included in the expansion is the violation of the inequalities given by Eq. (13). The validity of these inequalities is derived on the basis of a variational principle which assumes completeness of the angular-momentum expansion. If the contributions of only one or two channels in the expansion closely represent the minimum of the potential curve, then the inequalities remain valid even when truncation is performed. However, if convergence is not achieved in the expansion, then the completeness requirement is not even approximately fulfilled, and the inequalities are violated.

Figure 2 shows the potential curves for several different semiconductors having different electron-hole mass ratios. The overall depth and location of the minima of these curves vary in a uniform fashion with respect to the ratio m of the hole mass to the electron mass. In particular, a detailed study of this variation yields the re-

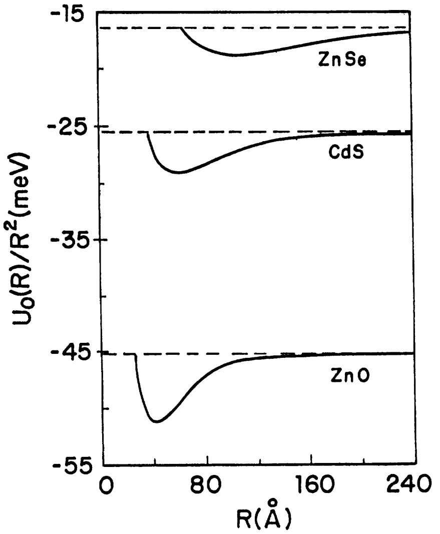

FIG. 2. Potential curves for selected semiconductors having different effective masses. The limits for large R correspond to the donor energies E_D when the hole is moving freely.

sult that there is a nearly linear relationship between both R and $U_0(R)/R^2$ at $R = R_{\rm min}$ and m. The influence of this behavior will be apparent in the results obtained for the binding energies in the next section.

IV. BOUND STATE ENERGIES AND WAVE FUNCTIONS

In the EAA the radial equations, Eq. (9), reduce to a single uncoupled equation for each of the curves $U_\lambda(R)$ of interest. Using potential curves $U_\lambda(R)$, of the type given in Fig. 1 as input to Eq. (9), we calculated binding energies in the EAA. Table I gives the results that we have obtained for several prominent semiconductors. A comparison of our results with earlier variational calculations is also given. We note that in all cases, the binding energies are a small fraction of the threshold energy if we compare them with realistic molecular systems like $H_2{}^+$ or $D_2{}^+$. This places considerable demands on the requirements for saturation in the angular-momentum expansion. In fact, in the case of InSb, the sample with the heaviest-hole mass ratio, the result violates the inequality expressed in Eq. (13). It is, indeed, higher than the 10.30% clearly signaling lack of convergence in the expansion.

When this HC method is compared to other approaches with regard to the influence of the hole mass, we see that it is, in some sense, complementary to the variational approach. In the HC case, larger hole masses require the inclusion of more angular-momentum components, thereby introducing difficulties and increasing errors. In a typical variational calculation, the region most difficult to handle is the region closer to the instability (light-hole mass) in which the expansion basis must contain both bound and scattering states. The last two columns can then be interpreted in light of Eq. (13) as establishing limits for the lower and upper bounds, respectively, on the binding energies. Within the limitations of the HC method, however, the calculated energies agree reasonably well with both the experimental and the theoretical results. The binding energies as a function of the mass ratio m in Fig. 3 are plotted. The energies are given as percentages of the binding energy of the donor in the limit of large R for the potential curve. For large values of m the system approaches that of the $H_2{}^+$ molecule. For the range of values $2 \leq m \leq 6$ corresponding to the common semiconductors, the fractional binding energy shows a very nearly linear variation with respect to m. For values smaller than 2.0, the fractional binding energy drops abruptly. This implies that other interactions which have been neglected in this calculation will likely perturb the system and can cause dissociation. Thus, bound states having energy this low may not be observed experimentally in semiconductors having holes of small mass.

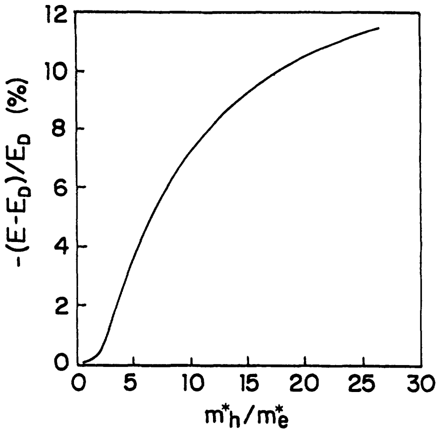

FIG. 3. Binding energy of the exciton-ionized donor complex as a function of the hole-electron mass ratio. E_D is the energy of the donor when the hole is at $R = \infty$.

The occurrence of bonding of the exciton to the ionized impurity is intimately connected to the value of the mass ratio m. This is easy to visualize when one notes that the bonding of the exciton to the ionized impurity will lead to a localization of the wave function in the region of the center. As the bonding is largely determined by the correlation between the electron and the hole, this wave function will have a much greater extent than is generally the case for the ground states of the atomic systems. As the mass of the hole increases, a transition takes place from a local mass region, in which the molecular behavior is dominant, to a delocalized sector, in which the wave function is spread. In order to understand the delocalization pattern, we have plotted in Fig. 4 the radial wave function $|F_0(R)|^2$ for several values of m. As m decreases, the maximum value of the wave function is lowered, and it tends to spread to larger values of R. Another way of looking at this behavior is given in Fig. 5, in which the mean value of the hyperspherical values, $\langle R \rangle$, is plotted as a function of m. For small values of m

TABLE I. Binding energies for several semiconductors. E_D is the dissociation energy. The indices refer to variational calculations. The static dielectric constants ϵ are taken from Ref. 3.

Material	ϵ	m_e^* (amu)	m_h^* (amu)	m_e^*/m_h^*	E_D (meV)	$E - E_D$ (meV)		$(E-E_D)/E_D$ (%)	
InSb	16.80	0.02	0.30	0.067	0.9641	0.0893	0.0993[a]	9.26	10.30[a]
ZnSe	9.10	0.10	0.60	0.167	16.43	0.751	0.676[a]	4.57	4.12[a]
CdS	10.33	0.20	1.00	0.20	25.50	0.918	0.791[b]	3.60	3.10[b]
ZnO	8.50	0.24	1.14	0.21	45.19	1.514	1.220[b]	3.35	2.70[b]
CdSe	10.66	0.13	0.59	0.22	15.56	0.486	0.348[a]	3.12	2.23[a]

[a] See Ref. 3.

[b] See Ref. 4.

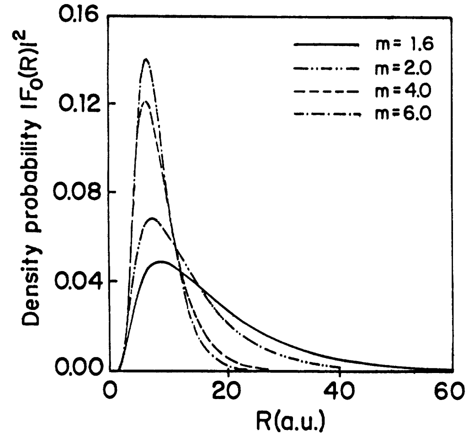

FIG. 4. Probability density $|F_\lambda(R)|^2$ for materials having different hole-electron mass ratios and the same dielectric constant. Note how the effect of the correlation distends the wave function as the hole mass become lighter.

the mean value increases sharply, while for larger values of m the mean value approaches a constant value, in keeping with the anticipated molecular like behavior. For $m=5$, the Coulombic system reaches its minimum size. This corresponds to the m value close to that for those semiconductors for which bound excitons have been observed.

Several values for the so-called "critical mass" at which bond formation will occur are found in the literature.[1,2,22,23] It seems that the concept of a critical mass is inextricably linked to the accuracy with which the calculation can be performed in the mass region around the critical mass.

We should also mention here the effect of the nonadiabatic couplings. The inclusion of the $W_{\lambda\lambda'}(R)$ terms [see Eq. (10)] will certainly increase the binding energy. It will certainly make quantitative changes in the other observables as a function of m. However, the basic arguments discussed above are, of course, not dependent on the inclusion of such nonadiabatic corrections but on the analytical properties of our equations.

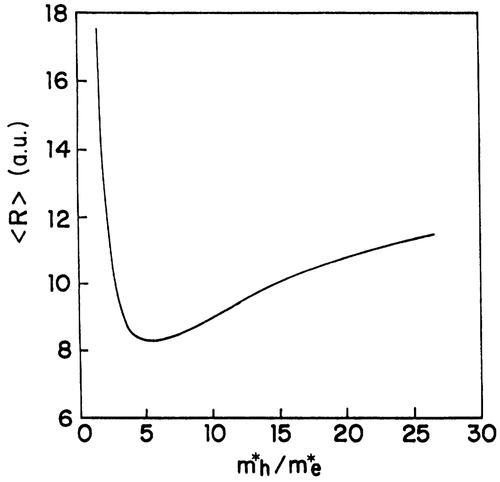

FIG. 5. Mean value of the hyperspherical radius in the effective atomic unit defined in the text. For small values of the mass ratio the size of the system increases drastically. Most of the semiconductors lie near the minimum of this curve.

V. CONCLUSIONS

In this work we have shown that the mathematical approach of the use of hyperspherical coordinates in the adiabatic approximation (HAA) is successful in describing excitons bound to imperfections in semiconductors even though the bonding is weak. The results that we obtain in the simplest EAA approach to the calculation are in very good agreement with variational calculations for several semiconductor materials. In light of the fact that the binding energies calculated in the EAA should represent a lower bound for the ground-state energy of the system, our results are a determination of this lower bound for a number of semiconductors. Only for those semiconductors for which the truncation of angular-momentum channels included in the calculation limits convergence is the inequality equation (13) not valid. For this case the EAA result is not a lower bound.

The concept of an overall size of the bound state contained in the definition of the hyper-radius R allows us to describe the bond formation through the localization of the hole and electron in the vicinity of the impurity. This overall size is shown to be dependent on the ratio m of the mass of the hole to that of the electron. This behavior is clearly illustrated in the behavior of the binding energies (Fig. 3) and the mean value of the hyper-radius $\langle R \rangle$ (Fig. 5) as a function m. It is apparent from the localized behavior of the wave functions, as illustrated in Fig. 4, that bonding is possible for any value of the mass ratio m. This seems to imply that the emergence of a critical mass beyond which bonding cannot occur is an artifact of the computational accuracy and is not a fundamental limitation imposed by the physics of the problem. What appears in the calculation as a type of critical mass is actually a minimum in the size of the bound state, as reflected in the value of $\langle R \rangle$ at a specific value of m.

This approach to the use of hyperspherical coordinates in the calculation of bonding of excitons to charged impurities has been performed with all radial coupling terms neglected. Currently, more precise calculations including these terms are underway. While we anticipate that the results obtained with these terms included should be more accurate, the general behavior of the bonding and the localization should not be significantly altered. In particular, we expect the conclusion on the nonexistence of a critical mass to be unaffected by more accurate calculations that will be performed.

ACKNOWLEDGMENTS

One of the authors (H.T.C.) would like to thank Dr. Y. Nogami for useful discussions and the kind hospitality received at McMaster University where part of the manuscript was written. We would also like to thank Dr. M. Degani and Dr. O. Hipólito for useful discussions. This work was partially supported by Conselho Nacional de Desenvolvimento Científico e Tecnológico (CNPq), Fundação de Amparo à Pesquisa de São Paulo (FAPESP), Fundação de Amparo à Ciência e Tecnologia de Pernambuco (FACEPE), e Financiadora de Estudos e Projetos (FINEP) (Brazilian agencies).

APPENDIX A: THE HYPERSPHERICAL COORDINATES

Jacobi coordinates is an appropriate set for the three-body problem. Let $\mathbf{r}_i$ be the coordinate of particle i in the laboratory frame, which has mass m_i. Let ρ_1 be the vector from particle 1 to particle 2 with reduced mass

$$\mu_1 = m_1 m_2/(m_1+m_2) \ .$$

The second vector ρ_2 is from the center of mass (c.m.) of particles 1 and 2 to particle 3, with reduced mass

$$\mu_2 = (m_1+m_2)m_3/(m_1+m_2+m_3) \ .$$

This procedure can easily be generalized to N-body systems.[14] It is also useful to introduce a set of mass-weighted coordinates $\xi_i = (\mu_i/\mu)^{1/2}\rho_i$, where μ is an arbitrary mass. The choice of Jacobi coordinates is not unique,[14] but normally dictated by the nature of the physical problem under consideration.

We can explicitly write down our choice of coordinates, used in this work, as

$$\begin{aligned} \xi_0 &= (m_1\mathbf{r}_1+m_2\mathbf{r}_2+m_3\mathbf{r}_3)/(m_1+m_2+m_3) \ , \\ \xi_1 &= (\mu_1/\mu)^{1/2}(\mathbf{r}_1-\mathbf{r}_2) \ , \\ \xi_2 &= (\mu_2/\mu)^{1/2}\left[\frac{m_1\mathbf{r}_1+m_2\mathbf{r}_2}{m_1+m_2}-\mathbf{r}_3\right] \ . \end{aligned} \tag{A1}$$

The Hamiltonian of our three-body system interacting via Coulomb forces is written as

$$\begin{aligned} H = &-\frac{\hbar^2}{2(m_1+m_2+m_3)}\nabla^2_{\xi_0}-\frac{\hbar^2}{2\mu}(\nabla^2_{\xi_1}+\nabla^2_{\xi_2}) \\ &+V(\xi_1,\xi_2) \ , \end{aligned} \tag{A2}$$

where

$$\begin{aligned} V(\xi_1,\xi_2) = &\left[\frac{\mu_1}{\mu}\right]^{1/2}\frac{q_1q_2}{\epsilon\xi_1}+\frac{m_1}{\sqrt{\mu\mu_1}}\frac{q_1q_3}{\epsilon|\xi_1+\eta_+\xi_2|} \\ &+\frac{m_2}{\sqrt{\mu\mu_1}}\frac{q_2q_3}{\epsilon|\xi_1-\eta_-\xi_2|} \ , \end{aligned} \tag{A3}$$

and

$$\begin{aligned} \eta_+ &= [m_1(m_1+m_2+m_3)/m_2m_3]^{1/2} \ , \\ \eta_- &= [m_2(m_1+m_2+m_3)/m_1m_3]^{1/2} \ . \end{aligned} \tag{A4}$$

The symbol q_i stands for the particle electric charges and ϵ for the static dielectric constant. Note that the use of Jacobi coordinates separated the c.m. motion in the kinetic energy operator. In this way we can consider only the resulting Schrödinger equation in the c.m. At this point it is appropriate to introduce hyperspherical coordinates by defining a hyperspherical radius R

$$R^2 = \xi_1^2+\xi_2^2 \ ,$$

and a hyperspherical angle α

$$\begin{aligned} \xi_1 &= R\sin\alpha \ , \\ \xi_2 &= R\cos\alpha, \quad 0\le\alpha\le\pi/2 \ . \end{aligned} \tag{A5}$$

The Schrödinger equation, $H\psi=E\psi$ in hyperspherical coordinates can be written as[12]

$$\left[\frac{\partial^2}{\partial R^2}-\frac{U(R,\Omega)-\frac{1}{4}}{R^2}+\varepsilon\right]\psi(R,\Omega)=0 \ , \tag{A6}$$

where $\Psi(R,\Omega)$ is the normalized wave function,

$$\Psi(R,\Omega)=R^{5/2}\sin\alpha\cos\alpha\,\psi(R,\Omega) \ ,$$

$\varepsilon=(2\mu/\hbar^2)E$, E being the energy eigenvalue, and

$$\Omega=\{\alpha,\hat{\xi}_1=(\theta_1,\varphi_1),\hat{\xi}_2=(\theta_2,\varphi_2)\} \ .$$

$U(R,\Omega)$, is given by

$$U(R,\Omega)=-\frac{\partial^2}{\partial\alpha^2}+\frac{\hat{l}_1^2(\hat{\xi}_1)}{\sin^2\alpha}+\frac{\hat{l}_2^2(\hat{\xi}_2)}{\cos^2\alpha}+R\hat{v}(\alpha,\theta) \ . \tag{A7}$$

The quantities $\hat{l}_i^2(\hat{\xi}_i)$ ($i=1$ and 2) stand for the usual angular-momentum operators. Defining $v=(2\mu/\hbar^2)V$, and $V(R,\Omega)=\hat{V}(\alpha,\theta)/R$, where

$$\begin{aligned} \hat{V}(\alpha,\theta) = &\left[\frac{\mu_1}{\mu}\right]^{1/2}\frac{q_1q_2}{\epsilon\sin\alpha}+\frac{m_1}{\epsilon\sqrt{\mu\mu_1}}q_1q_3[\sin^2\alpha+\eta_+^2\cos^2\alpha+\eta_+\sin(2\alpha)\cos\theta]^{-1/2} \\ &+\frac{m_2}{\epsilon\sqrt{\mu\mu_1}}q_2q_3[\sin^2\alpha+\eta_-^2\cos^2\alpha-\eta_-\sin(2\alpha)\cos\theta]^{-1/2} \end{aligned} \tag{A8}$$

and $\cos\theta=\hat{\xi}_1\cdot\hat{\xi}_2$. Note that

$$\hat{v}(\alpha,\theta)=(2\mu/\hbar^2)\hat{V}(\alpha,\theta) \ .$$

APPENDIX B: EVALUATION OF THE CHANNEL-MIXING COEFFICIENTS

To calculate the matrix elements of v in Eq. (17), because of the form of Eq. (5), we first need to evaluate the tensor

$$\begin{aligned} \mathcal{T}^{LM}_{l_el'_el_hl'_h}(\alpha) = &\int d\hat{\xi}_e d\hat{\xi}_h \mathcal{Y}^{LM}_{l'_el'_h}(\hat{\xi}_e,\hat{\xi}_h)^* \\ &\times[\sin^2\alpha+\eta_-^2\cos^2\alpha-\eta_-\sin(2\alpha)\cos\theta]^{-1/2} \\ &\times\mathcal{Y}^{LM}_{l_el_h}(\hat{\xi}_e,\hat{\xi}_h) \ . \end{aligned} \tag{B1}$$

Notice that the square-root term can always be written in the form

$$f(1+t^2-2tx)^{-1/2}, \quad x=\cos\theta \;, \tag{B2}$$

where the expressions for f and t are given in Table II.

We also know by the definition of Legendre polynomials[21] that

$$(1+t^2-2tx)^{-1/2}=\sum_{L'=0}^{\infty} t^{L'}P_{L'}(x), \quad |t|<1 \;. \tag{B3}$$

Because of the selection rules used below, the condition $|t|<1$ is not mandatory. Using the addition theorem for $P_L(x)$ and the fact that

$$\mathcal{Y}_{l_el_h}^{LM}(\hat{\xi}_e,\hat{\xi}_h)=\sum_{m_e,m_h}\langle LM|l_em_el_hm_h\rangle \times Y_{l_em_e}(\hat{\xi}_e)Y_{l_hm_h}(\hat{\xi}_h) \;, \tag{B4}$$

we obtain, after some straightforward algebra, the expression

$$\begin{aligned}\langle\hat{v}\rangle = &-\left[\frac{m_e^*}{\mu}\right]^{1/2}\frac{Ze^2}{\epsilon\sin\alpha}\delta_{l_el_e'l_hl_h'} \\ &+\left[\frac{m_h^*}{\mu}\right]^{1/2}\frac{Ze^2}{\epsilon\cos\alpha}\delta_{l_el_e'l_hl_h'} \\ &-\left[\frac{m_e^*}{\mu}\right]^{1/2}\frac{e^2}{\epsilon}\Delta_{l_el_e'l_hl_h'}(\alpha) \;,\end{aligned} \tag{B5}$$

TABLE II. Expressions for t and f appearing in Eq. (B2).

α interval	f	t
$0\le\alpha\le\alpha_c$	$(\eta_-\cos\alpha)^{-1}$	$\tan\alpha/\eta_-$
$\alpha_c\le\alpha\le\pi/2$	$(\sin\alpha)^{-1}$	$\eta_-\cot\alpha$

where

$$\Delta_{l_el_e'l_hl_h'}(\alpha)=\sum_{L'}(-1)^{L'}C_{l_el_e'l_hl_h'}^{LL'}\mathcal{D}_{L'}(\alpha) \;, \tag{B6}$$

and

$$C_{l_el_e'l_hl_h'}^{LL'}=(-1)^{L+L'}[(2l_e+1)(2l_e'+1)(2l_h+1) \times(2l_h'+1)]^{1/2} \times\begin{pmatrix} l_e & l_e' & L' \\ 0 & 0 & 0\end{pmatrix}\begin{pmatrix} l_h & l_h' & L' \\ 0 & 0 & 0\end{pmatrix}\begin{Bmatrix} l_e & l_h & L \\ l_h' & l_e' & L'\end{Bmatrix} , \tag{B7}$$

where the usual 3-j and 6-j symbols appear. The $\mathcal{D}_{L'}$ terms are given by

$$\mathcal{D}_{L'}(\alpha)=\begin{cases}(\tan\alpha/\eta_-)^{L'}(\eta_-\cos\alpha)^{-1}, & 0\le\alpha\le\alpha_c \\ (\eta_-\cot\alpha)^{L'}/\sin\alpha, & \alpha_c\le\alpha\le\pi/2 \;,\end{cases} \tag{B8}$$

where $\tan\alpha_+=+\infty$ and $\tan\alpha_-=\tan\alpha_c=1/\sqrt{m}$. In terms of the variable z, $\mathcal{D}_{L'}(z)$ can easily be obtained by noticing that $\tan\alpha=2z/(1-z^2)$, $\cot\alpha=(1-z^2)/2z$, $(\sin\alpha)^{-1}=(1+z^2)/2z$, and $(\cos\alpha)^{-1}=(1+z^2)/(1-z^2)$.

---

[1] J. J. Hopfield, in *Proceedings of the Seventh International Conference on the Physics of Semiconductor, Paris, 1964* (Dunod, Paris, 1964), p. 725; S. Schmitt-Rink, D. S. Chemla, and D. A. B. Miller, Adv. Phys. **38**, 89 (1989), and references therein.

[2] R. R. Sharma and S. Rodriguez, Phys. Rev. **153**, 823 (1967).

[3] M. Suffczynski, W. Gorzkowski, and Kowalczyk, Phys. Lett. **24A**, 453 (1967).

[4] T. Skettrup, M. Suffczynski, and W. Orzkowski, Phys. Rev. B **4**, 512 (1971).

[5] H. J. Wunshe and K. Henneberger, Phys. Status Solidi B **91**, 336 (1979).

[6] B. Stébé and L. Stauffer, Superlatt. Microstruct. **5**, 451 (1989).

[7] D. G. Seiler, K. H. Littler, and C. L. Littler, Semicond. Sci. Technol. **1**, 383 (1986).

[8] E. Finkman, M. D. Sturge, and R. Bhat, J. Lumin. **35**, 235 (1986).

[9] T. Takagahara, Phys. Rev. B **39**, 10 206 (1989).

[10] D. A. B. Miller, Int. J. High Speed Electron. **1**, 19 (1989).

[11] Al. L. Éfros and A. L. Éfros, Fiz. Tekh. Poluprovodn. **16**, 1209 (1982) [Sov. Phys. Semicond. **16**, 772 (1982)].

[12] H. T. Coelho, T. K. Das, and M. R. Robilotta, Phys. Rev. C **28**, 1812 (1983); T. K. Das, H. T. Coelho, and M. Fabre de la Ripelle, *ibid.* **26**, 2281 (1982).

[13] J. E. Hornos, S. W. Mac Dowell, and C. D. Caldwell, Phys. Rev. A **33**, 2212 (1986); H. T. Coelho, J. J. de Groote, and J. E. Hornos (unpublished).

[14] C. D. Lin and Xian-Hu Liu, Phys. Rev. A **37**, 2749 (1988).

[15] C. D. Lin, Adv. Mod. Phys. **22**, 77 (1986).

[16] J. H. Macek, J. Phys. B **1**, 831 (1968).

[17] V. P. Brito, H. T. Coelho, and T. K. Das, Phys. Rev. A **40**, 3346 (1989); S. K. Adhikari, V. P. Brito, H. T. Coelho, and T. K. Das, Nuovo Cimento (to be published).

[18] C. H. Greene, Phys. Rev. A **23**, 661 (1981); V. Fano, Rep. Prog. Phys. **46**, 97 (1983).

[19] H. T. Coelho and J. E. Hornos, Phys. Rev. A **43**, 6379 (1991).

[20] Yu. F. Smirnov, and K. V. Shitikova, Fiz. Elem. Chastits At. Yadra, **8**, 847 (1977) [Sov. J. Part. Nucl. **8** (4), 344 (1977)].

[21] *Handbook of Mathematical Functions,* edited by M. Abranowitz and I. A. Stegun, 3rd ed. (Dover, New York, 1965).

[22] Tsin-Fu Jiang, Solid State Commun. **74**, 899 (1990).

[23] F. H. Gertler, H. B. Snodgrass, and L. Spruch, Phys. Rev. **172**, 110 (1968).